Final Report NAG-1-798

NUMERICAL SIMULATION OF PARTICLE-WAVE INTERACTION IN BOUNDARY LAYERS

S. Biringen and G. Danabasoglu
Department of Aerospace Engineering Sciences
University of Colorado, Boulder, CO 80309

1. OBJECTIVES OF THE RESEARCH

The computational work described in this report describes the preliminary results concerning the interaction of instability waves with a moving source of vorticity in boundary layer flow. The importance of the problem stems from the fact that as an underwater vehicle moves through a particulate environment, particles enter the boundary layer and produce local instabilities. These instabilities may lead to turbulent events by themselves or they may interact with Tollmien-Schlichting waves and act as amplifiers to enhance the instability. The effects of a particle on boundary layer instability may manifest itself in several different forms:

(a) receptivity and by-pass transition,

(b) blockage and mean velocity modification.

During the first phase of this research program, we focused on the blockage effect and considered the two-dimensional channel flow as the model problem. The approach used in the present work consists of the following main elements:

(a) Use of the full, three-dimensional, unsteady Navier-Stokes equations (Ref.1)

(b) Incorporation of accurate inflow-outflow boundary conditions to capture the true spatially-evolving nature of the problem.

(c) The time-accurate numerical integration of the governing equations with a spectral method.

The code was applied to several different configurations outlined below:

(a) The generation of a local disturbance at a fixed, specifed location in the flow and the determination of its evolution in space and time.

(b) The generation of a disturbance by a particle moving through the flow along a prescribed path.

In both of the above cases, the particle was assumed to create a vorticity disturbance which was computationally generated by alternate suction/blowing. The results are presented in

the following section and emphasize the evolution of Tollmien-Schlichting (TS) waves before and after their interaction with the particle-generated vortical disturbance..

2. RESULTS

In this section, we discuss the effects of wall injection and particle motion on the spatial stability of two-dimensional plane channel flow. For all the calculations, the Reynolds number and the frequency were set to Re=5000 and ω=0.33017, respectively, resulting in a subcritical disturbance for the two dimensional Poiseuille flow. First, the fully-developed channel flow is disturbed by a two-dimensional perturbation imposed at the inflow. These perturbation velocities were obtained from the solution of the nonlinear Orr-Sommerfeld equation and their maximum amplitude was set to 0.0011 (0.11% of the channel centerline velocity) simulating a low amplitude, linear disturbance which slowly decays at the subcritical Reynolds number, Re=5000. After the flow reaches a quasi-steady state, the wall injection or particle motion is started. In all the numerical experiments, a 41x129 grid is used in the physical domain; the length of the streamwise direction (x) is 16 in the physical domain and contains approximately three wavelengths of the spatially developing wave.

First, we investigate the effects of wall injection. For this purpose, the fluid is injected between x=6 and x=6.25 on the lower wall with the horizontal and vertical velocity components equal to 0.012 and 0.00012, respectively. In Fig.1, the numerically calculated amplitudes of the streamwise component of the perturbation velocity are compared with the linear exact solution at different vertical (y) locations. The coordinates of these locations are provided in Table 1, and they are the same for all the figures presented in this study. The plots in Fig.1 were obtained after three periods of the Tollmien-Schlichting (TS) wave and indicate that the amplitude of the perturbation velocity increases even near the upper wall in the downstream direction and the upstream effect becomes more pronounced as the wall injection region is approached. The perturbation streamfunction, vorticity and streamwise velocity contours are presented in Fig.2 showing the overall effects of the wall injection.

Next, the effects of particle motion are studied during a time period equal to two periods of the TS wave. For this calculation, one period was divided into 3000 time steps and the particle was allowed to slowly change its position and velocity at every 1000 time steps. The streamwise and normal ranges of the particle trajectory were [5.375,7.25] and

[-0.309,-1], respectively. Similarly, the horizontal and vertical perturbation velocity components of this moving disturbance were varied between [0.00012,0.0012] and [-0.00012,-0.000012], respectively. In Fig. 3, it is apparent that the effects of the moving disturbance on the amplitude distributions is much greater than the effect of wall injection (stationary source of disturbance) in both the upstream and downstream of the source. The frames in this figure also display a the small phase difference with the exact solution as well as the formation of a subharmonic in the last frame. These are indicative of nonlinear interactions and support the idea that the vorticity generated by the moving particle acts as an amplifier to enhance the growth of TS waves.

In order to investigate the effects of fast particle motion, we present a case in which the particle position and velocity are changed every 100 time steps. Here, the streamwise and normal ranges of the particle trajectory were set to [5.375,6.875] and [-0.522,-1], respectively, and the previous perturbation velocity magnitudes were employed. Figures 5 and 6 provide the results at time step 300 (at which the particle is close to the fifth vertical (y) location). In Fig. 5, it is observed that the effects of this perturbation is confined to the neighbourhood of the particle and to the lower half of the channel. After the particle reaches the lower wall, (Figs. 7 and 8), we note that the particle motion is felt mostly in the upstream direction and the amplitude and phase differences are not as pronounced as the previous slow particle motion case. Figures 6 and 8 further testify that the effects of the disturbances are felt in the lower half of the channel.

Finally, to test the limits of the computer code with the limited mesh resolution that was used in these calculations, we increased the streamwise component of the perturbation velocity by an order of magnitude and used the previous conditions (i.e. trajectory and velocity) for the particle motion. The results at time step 300 (Figs. 9 and 10) show that the upper half of the channel is affected and disturbances due to the particle motion have propagated in both the downstream and upstream directions. In Figs. 11 and 12, we note that the disturbances amplify very rapidly after the particle reaches the lower wall. The contour plots shown in Fig. 12 display a region of concentrated vorticity which resembles a wave packet.

3. CONCLUDING COMMENTS

The accomplishments of tthis research can be summarized as follows:

(a) An accurate Navier-Stokes solver to simulate the space-time evolution of disturbances in three-dimensional flows has been developed. The code is operational on the NASA Langley CRAY2 and be ported to any other supercomputer.

(b) The code has been tested extensively in tracking the spatial evolution of two-dimensional disturbances in plane channel flow and provided excellent agreement with the linear theory including at the inflow/outflow boundaries.

(c) Preliminary calculations have been performed to investigate the effects of stationary and moving sources of vortical disturbances simulating a particle traveling in the flow field. Our findings suggest that even at very low amplitudes, vortical disturbances act as amplifiers on the Tollmien-Schlichting waves promoting rapid instability. It is also found that slow moving particles are more dangereous than both stationary and fast moving particles for the same disturbance levels.

During the subsequent phases of this research we intend to undertake the following tasks:

(a) Inclusion of full three-dimensionality using small amplitude disturbances.

(b) Application of the model developed in the preliminary study to the Blausius boundary layer; investigation of receptivity by modifying the external stream due to the presence of the entering particle.

(c) Detalied flow visualization of the three-dimensional velocity field.

(d) Investigation of active control techniques to suppress the complex instability field.

References

Danabasoglu, G., Biringen, S. and Streett C.L., "Numerical Simulation of Spatially Evolving Instability," in Instability and Transition (Eds. M.Y. Hussaini and R.G. Voigt), 394-407, Springer (1990).

Table 1 Key for the Odd Numbered Figures

Figure	y location
a	0.9969
b	0.8910
c	–0.3090
d	–0.6494
e	–0.8910
f	–0.9877

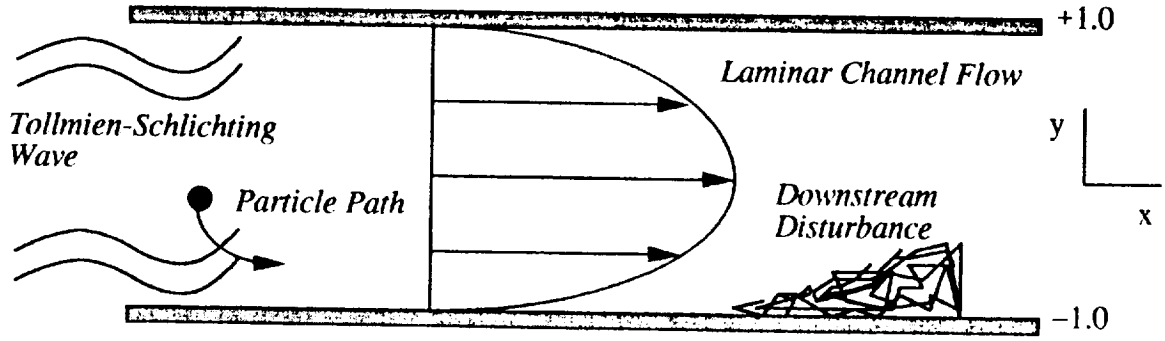

Schematic of the Flow

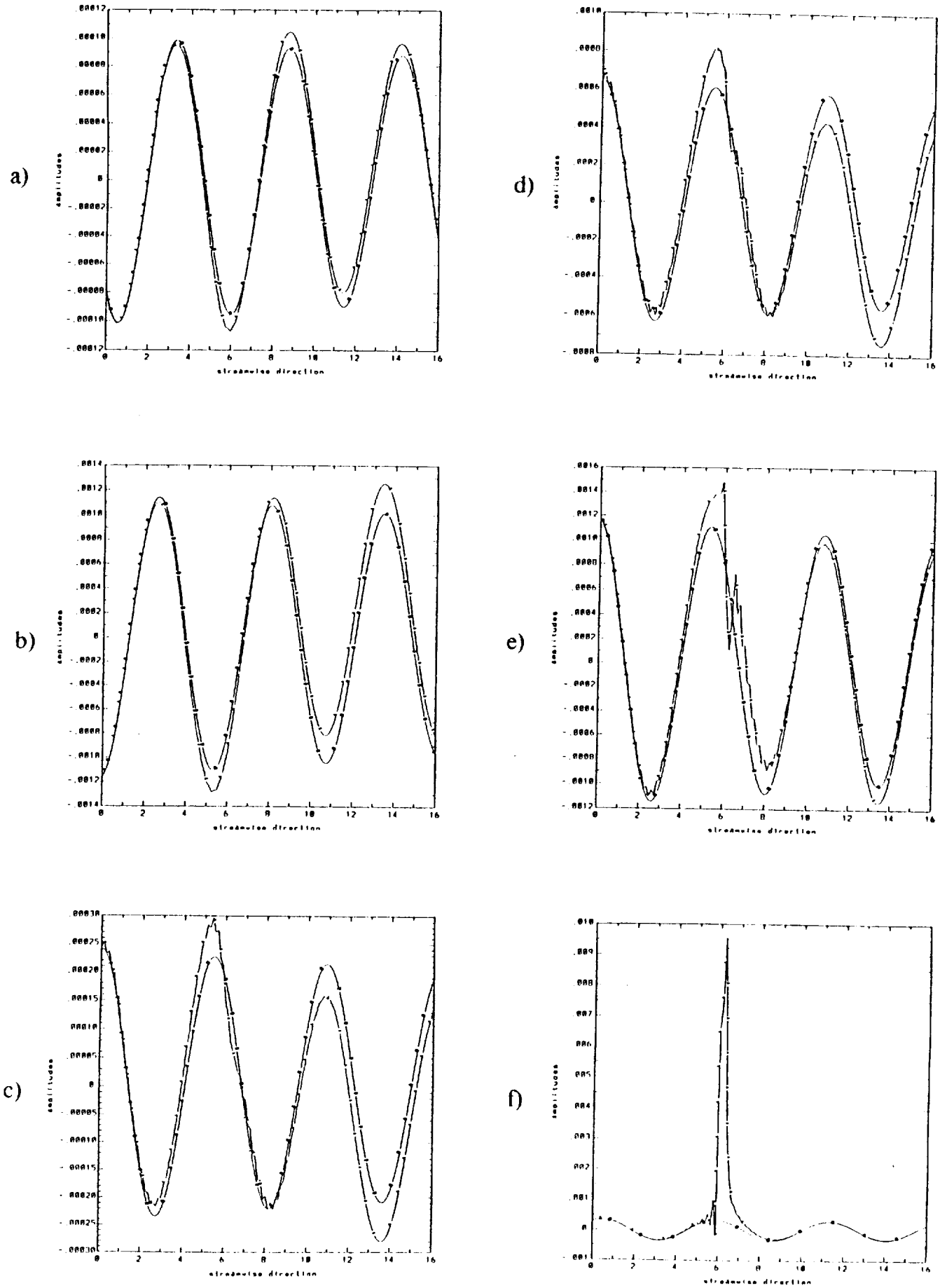

Figure 1. Comparison of the computed (A) streamwise perturbation velocity component with the linear exact (B) solution: wall injection (Re=5000,ω=0.33017).

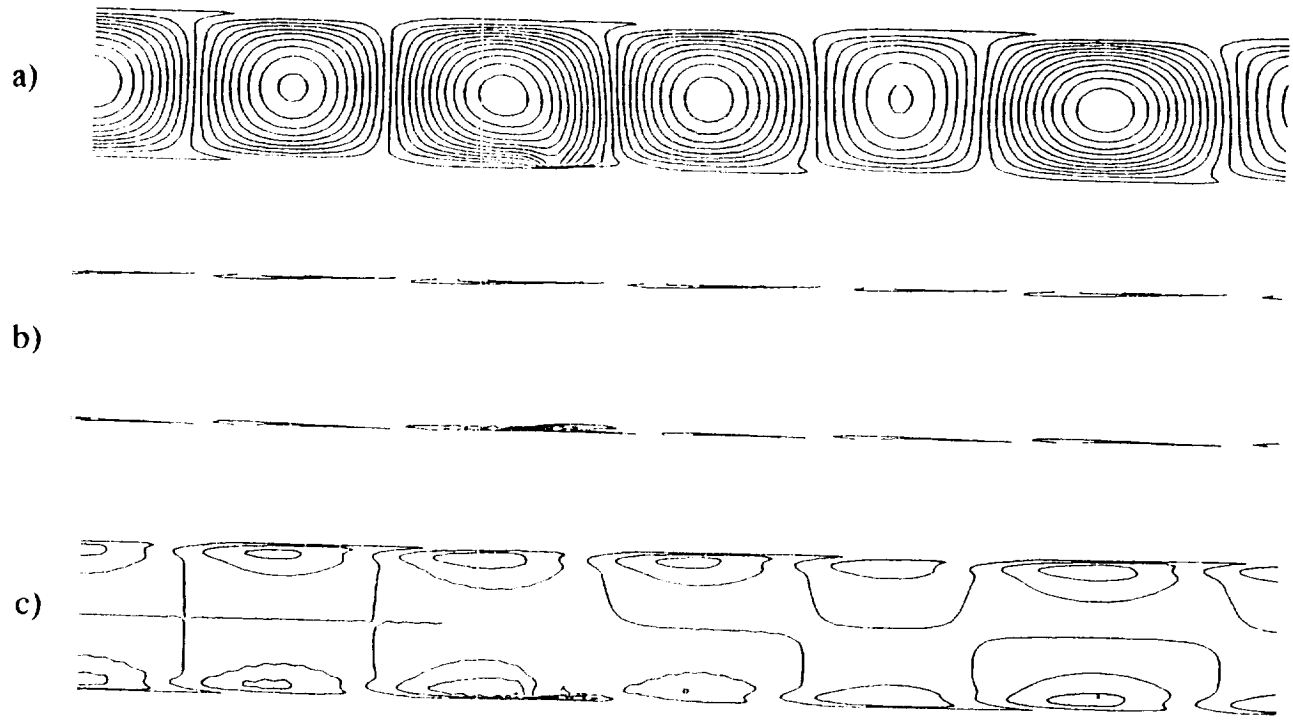

Figure 2. Perturbation streamfunction (a), vorticity (b) and streamwise velocity (c) contours for the case of Fig. 1 (Re=5000,ω=0.33017).

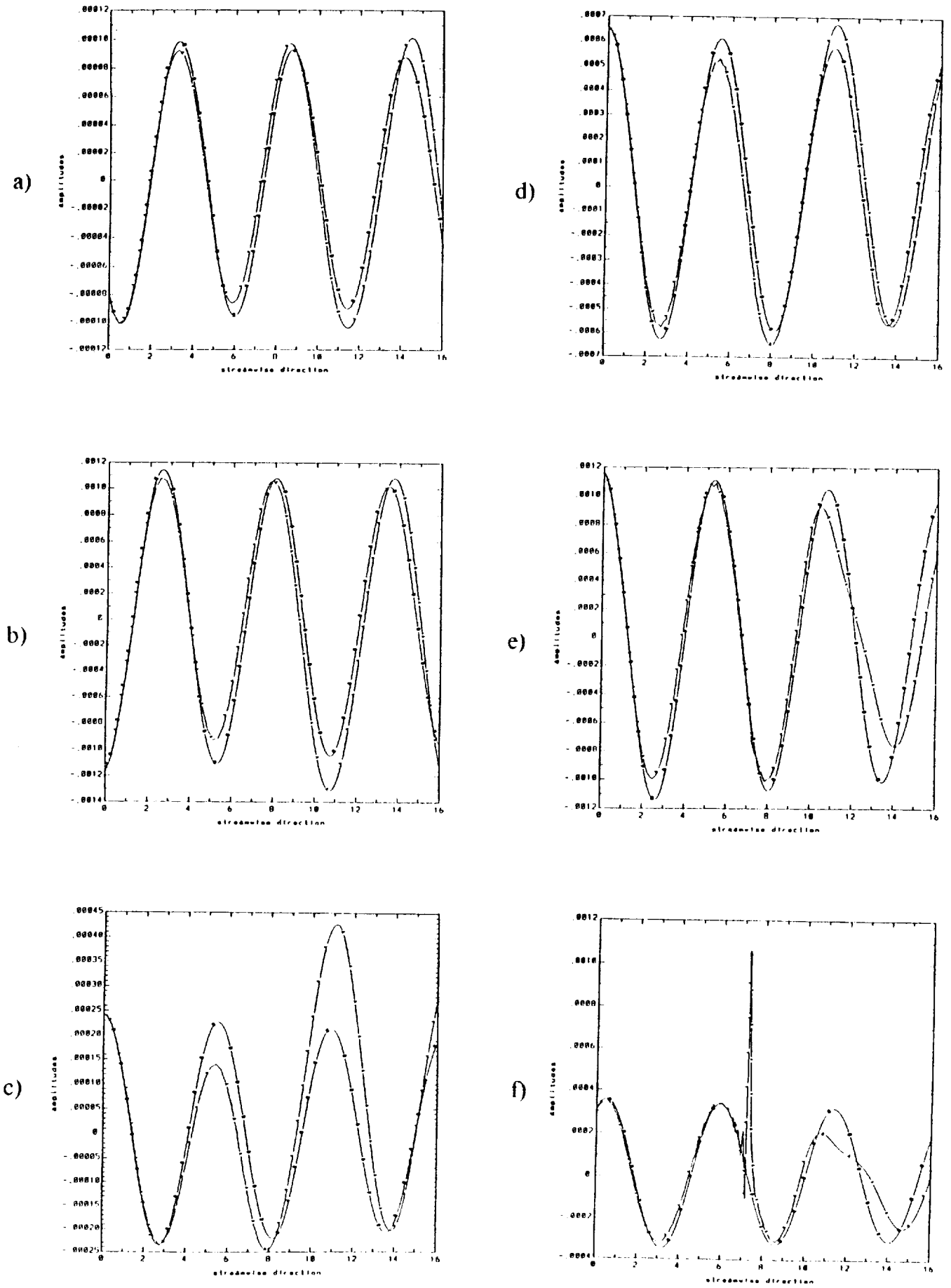

Figure 3. Comparison of the computed (A) streamwise perturbation velocity component with the linear exact (B) solution: slow particle motion (Re=5000,ω=0.33017).

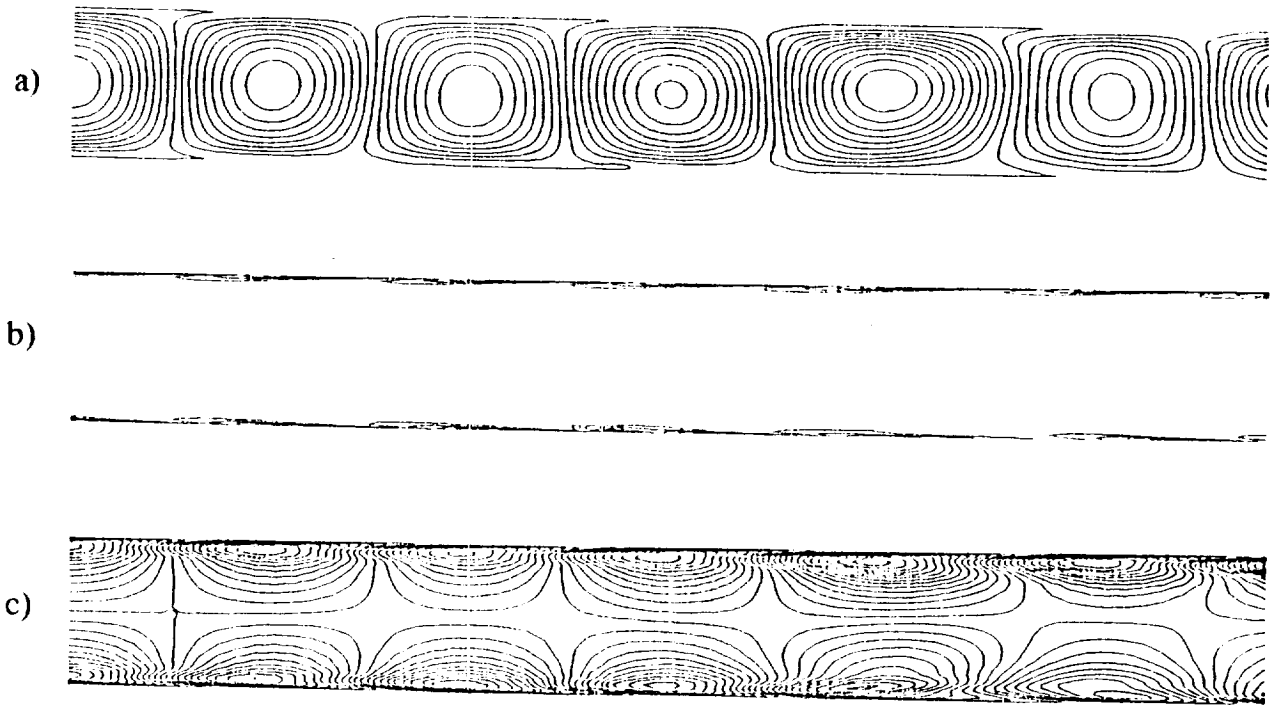

Figure 4. Perturbation streamfunction (a), vorticity (b) and streamwise velocity (c) contours for the case of Fig. 3 (Re=5000,ω=0.33017).

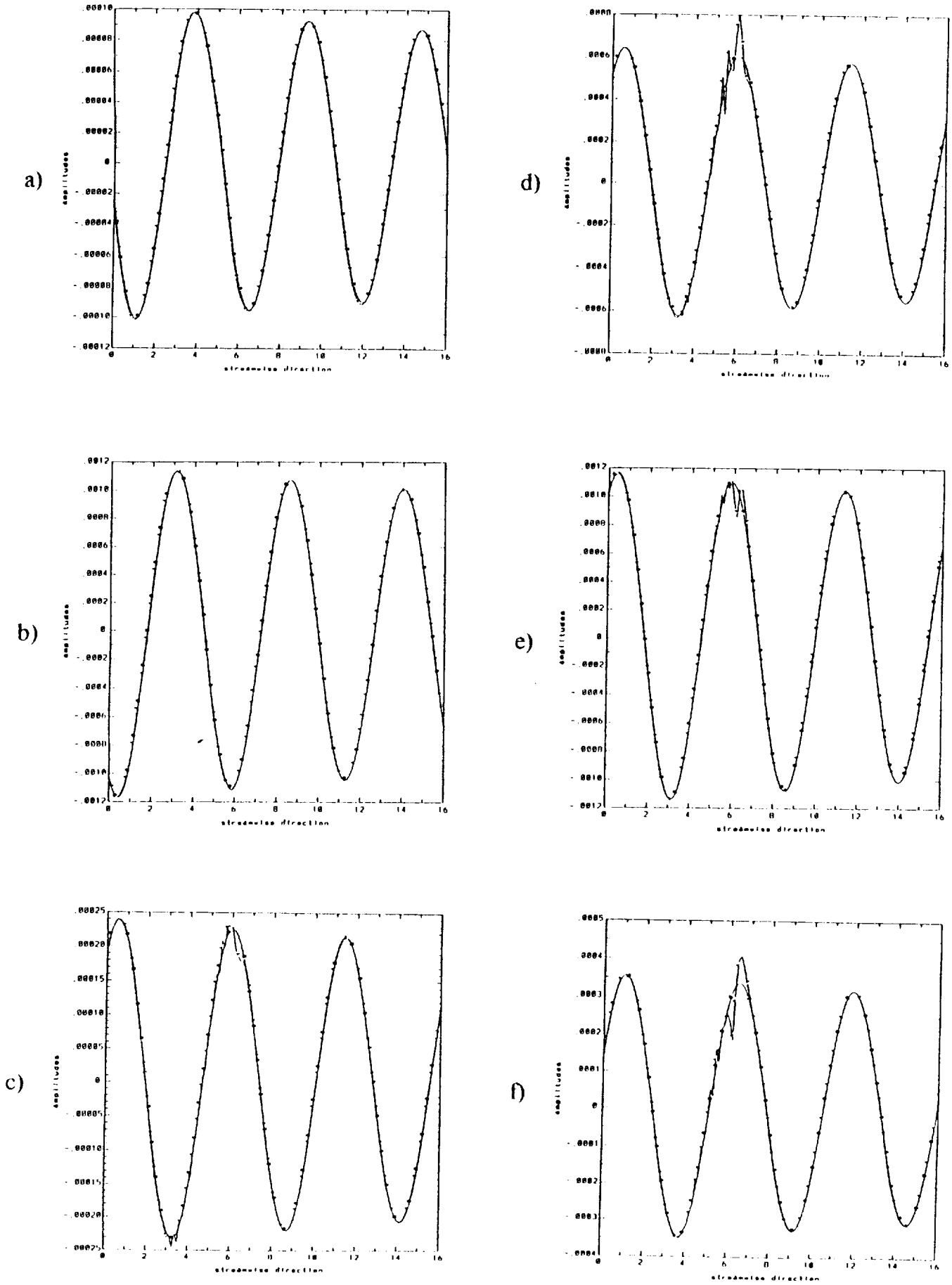

Figure 5. Comparison of the computed (A) streamwise perturbation velocity component with the linear exact (B) solution: fast particle motion - intermediate results (Re=5000,ω=0.33017).

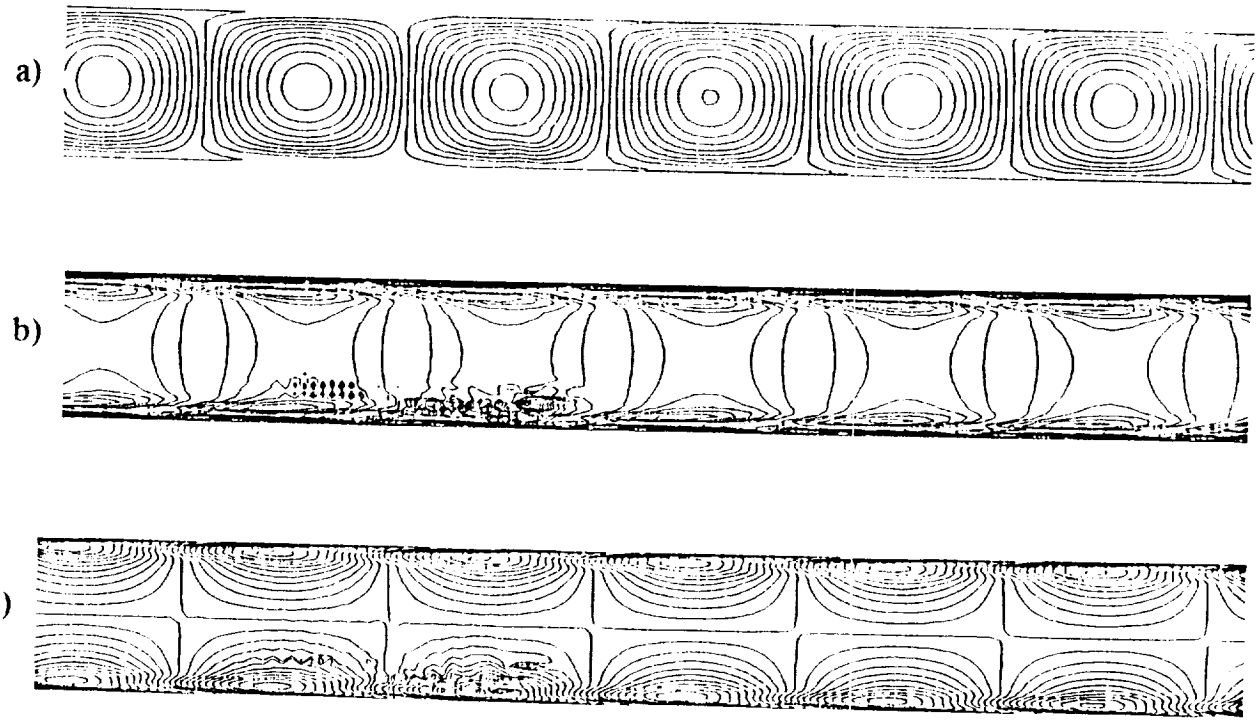

Figure 6. Perturbation streamfunction (a), vorticity (b) and streamwise velocity (c) contours for the case of Fig. 5 (Re=5000,ω=0.33017).

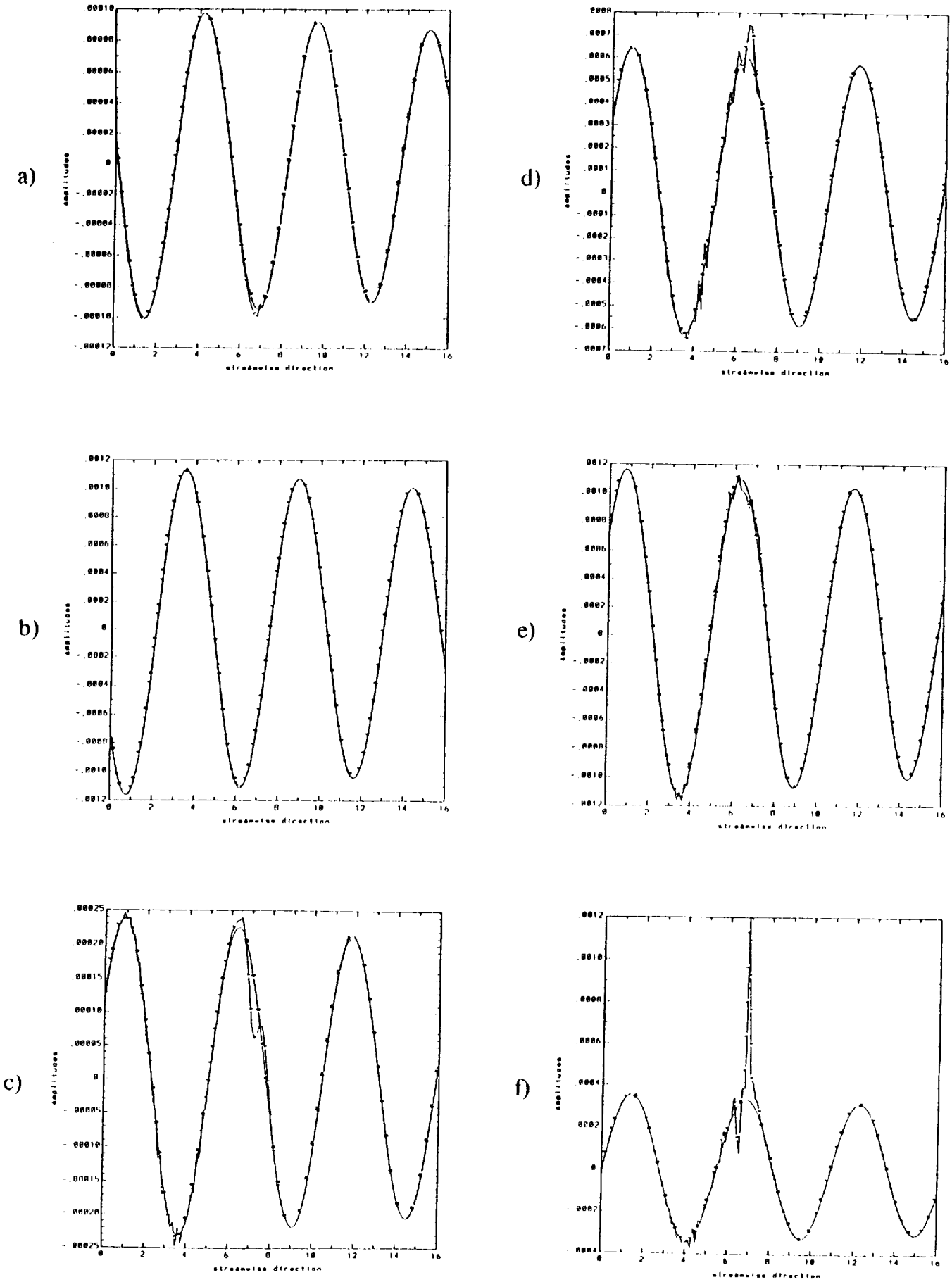

Figure 7. Comparison of the computed (A) streamwise perturbation velocity component with the linear exact (B) solution: fast particle motion (Re=5000,ω=0.33017).

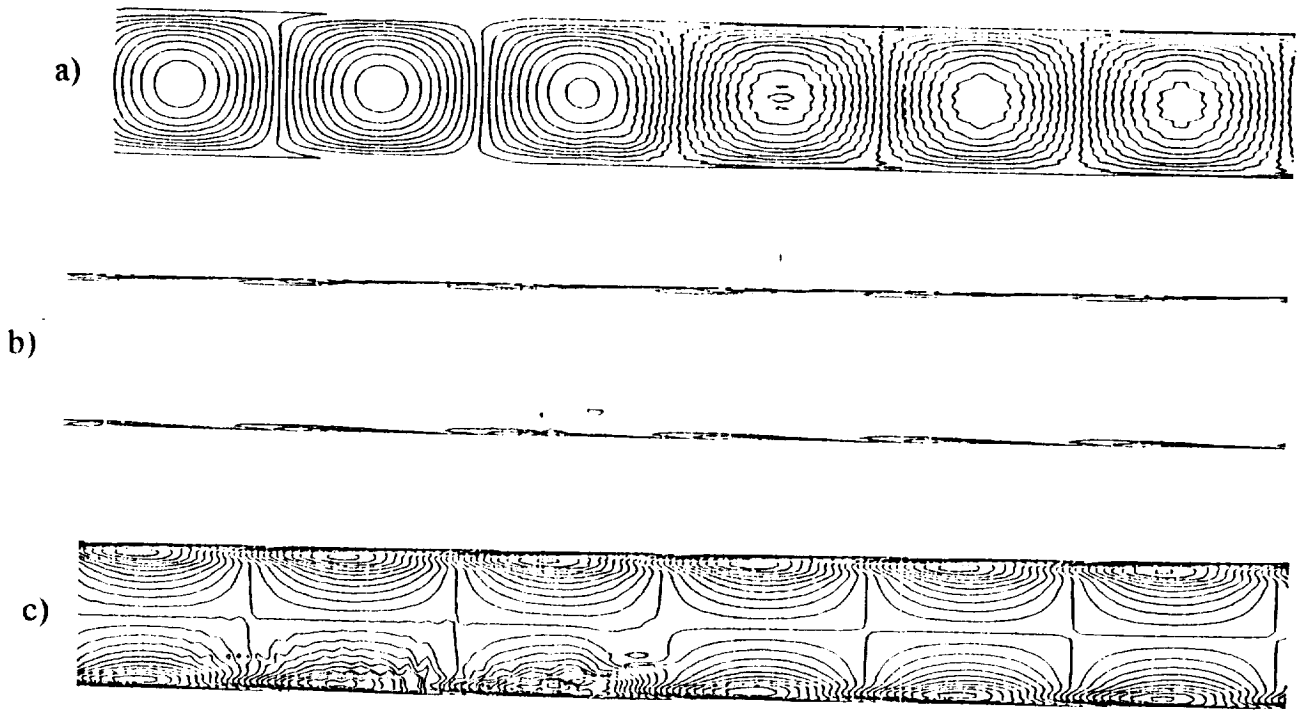

Figure 8. Perturbation streamfunction (a), vorticity (b) and streamwise velocity (c) contours for the case of Fig. 7 (Re=5000,ω=0.33017).

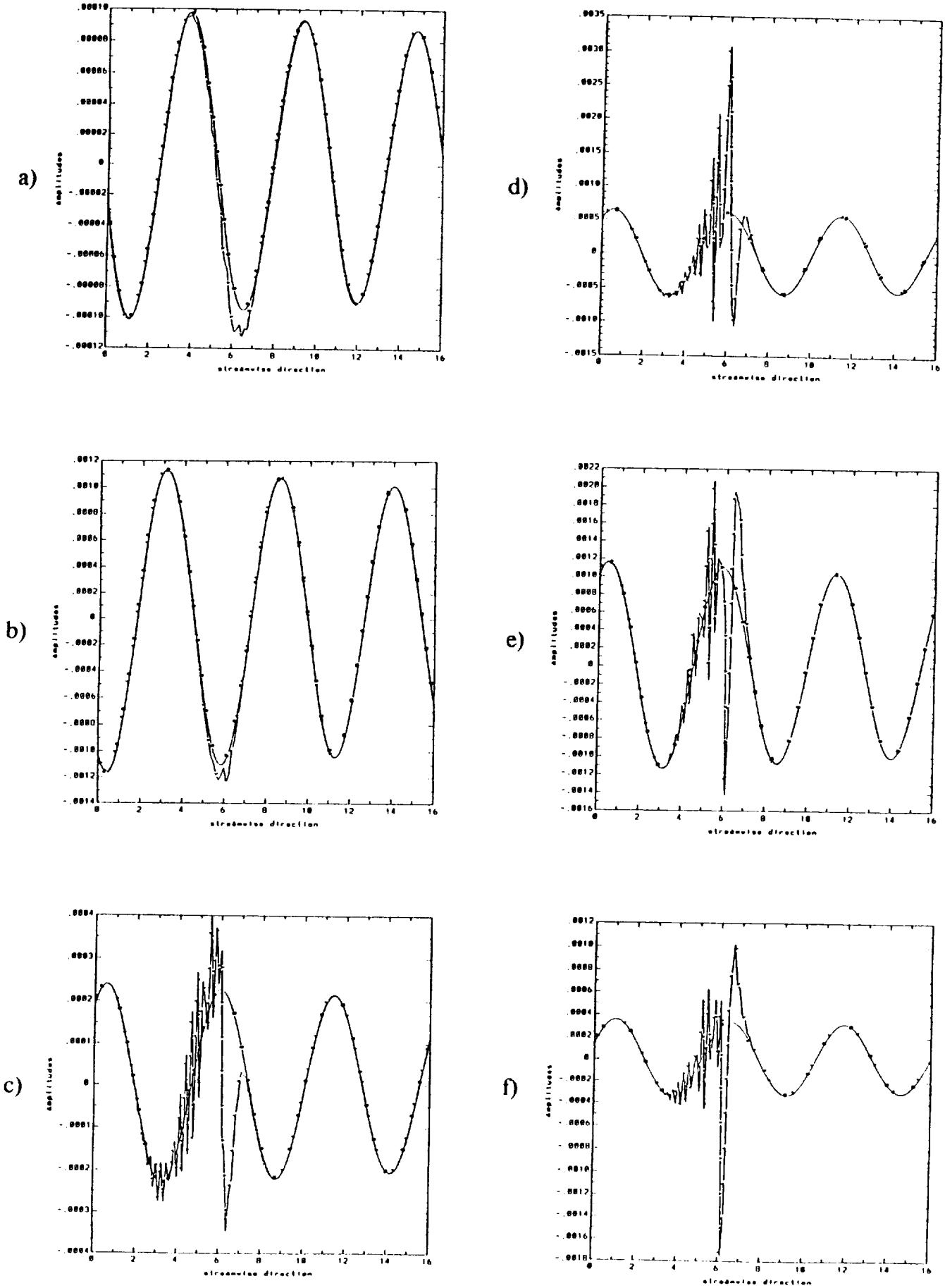

Figure 9. Comparison of the computed (A) streamwise perturbation velocity component with the linear exact (B) solution: fast particle motion with large streamwise perturbation velocity amplitude - intermediate results (Re=5000,ω=0.33017).

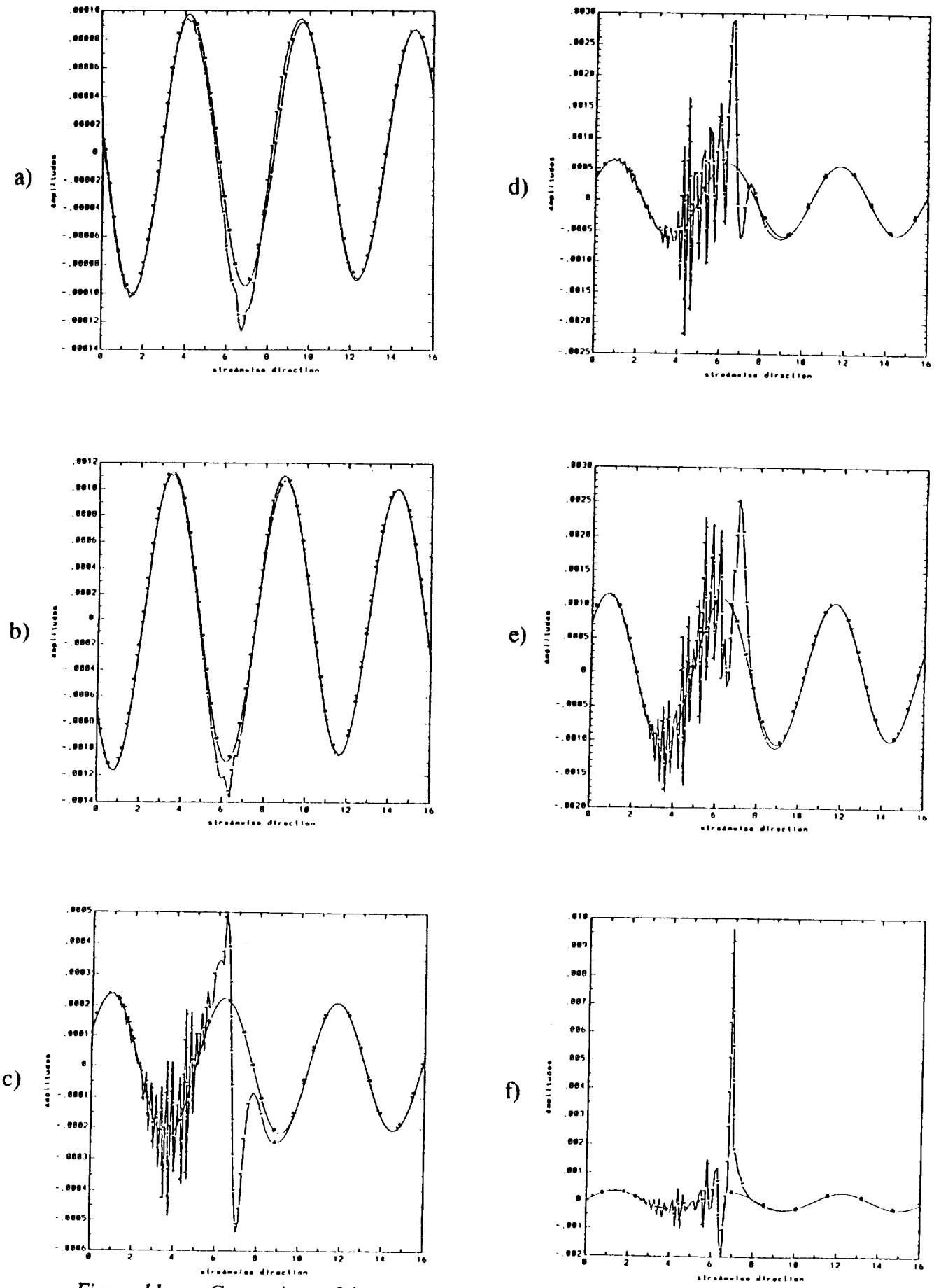

Figure 11. Comparison of the computed (A) streamwise perturbation velocity component with the linear exact (B) solution: fast particle motion with large streamwise perturbation velocity amplitude (Re=5000,ω=0.33017).

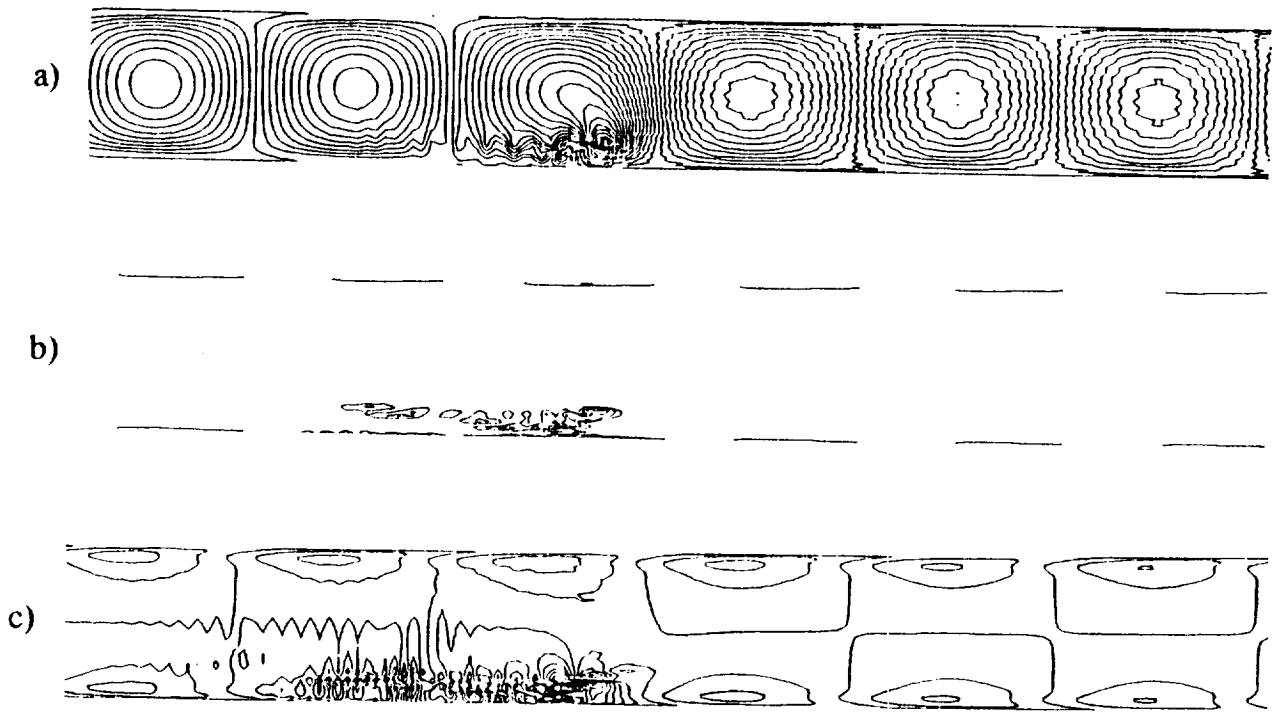

Figure 12. Perturbation streamfunction (a), vorticity (b) and streamwise velocity (c) contours for the case of Fig. 11 (Re=5000,ω=0.33017).